ARMA 15-781

Geomechanical rock mass characterization with Terrestrial Laser Scanning and UAV.

Tamburini, A.
Imageo Hortus Chile Ltda., Santiago, Chile
Martelli, D.C.G., Alberto, W., Villa, F.
Imageo Srl, Torino, Italy

This paper was prepared for presentation at the 49th US Rock Mechanics / Geomechanics Symposium held in San Francisco, CA, USA, 28 June-1 July 2015.

ABSTRACT: Thanks to the improvement of surveying equipments, i.e. Terrestrial Laser Scanners (TLS) and Unmanned Aerial Vehicles (UAV), dense point clouds and very precise 3D models of inaccessible rock cliffs can be obtained. Both commercial and self-developed data processing software packages allow the extraction of some parameters regarding discontinuity sets (i.e. orientation, intensity, Vb, etc.). Nevertheless, maps with the distribution of such parameters are still not common. A procedure for obtaining raster maps with the distribution of significant parameters for the geomechanical characterization of rock cliffs, open pit mine slopes and tunnel faces is presented in this paper. Some selected case studies in the Italian Alps will be presented.

1. INTRODUCTION

Thanks to the improvement of surveying equipment and data processing software, an increasing use of TLS (Terrestrial Laser Scanning) for investigating and monitoring rock cliffs has been made during the last decade (Figure 1).

Fig. 1. TLS survey of a rock cliff.

Both scanning speed and operational range have been significantly increased, reducing the surveying time and increasing the extension of the study areas.

Fig. 2. Aermatica ANTEOS UAV equipped with digital optical and thermal cameras.

More recently, professional UAVs (Unmanned Aerial Vehicles) equipped with optical and thermal cameras (Figure 2) as well as laser scanners became available, making it possible to integrate co-registered TLS and UAV data into a unique 3D software environment,

reducing shadow areas and providing very detailed 3D models of inaccessible rock cliffs with an accuracy of few centimeters.

By applying proper software packages, it's now possible to extract not only the attitude of rock mass discontinuity surfaces directly from the point cloud, but also to map the distribution of significant parameters influencing the behavior of the rock mass, e.g. frequency, spacing, P21 (cumulative tracelength per unit area), Vb (elementary rock volume), etc. Moreover, the possibility of draping high-resolution digital images over either a point cloud or a 3D mesh derived from it enhances the resolution of the 3D model and the capability of extracting geometrical information from the surveyed surface.

A workflow based on the use of both commercial software and properly developed GIS tools aimed at producing 2D and 3D maps with the distribution of significant parameters relevant to rock mass classification will be described.

2. METHODOLOGICAL APPROACH

The procedure described in this paper was developed by exploiting both commercial processing tools and originally developed software integrated into a workflow capable of providing raster maps with the distribution of significant parameters for the geomechanical characterization of rock cliffs, open pit mine slopes and tunnel faces.

The starting point of the proposed methodology is the point cloud provided by terrestrial laser scanner, terrestrial or UAV photogrammetry. The choice of the most appropriate surveying technique depends on several factors, such as the morphology of the slope, the extension of the study area, its distance from the surveying points and other logistic constraints. Different techniques can be integrated in order to reduce shadow areas and obtain a 3D model as complete as possible. As an example, integration between UAV photogrammetry and terrestrial laser scanning can be effectively applied when surveying stepped-ledge slopes.

The processing workflow is summarized in Figure 3. While 3D processing tools are provided by commercial software products (some of them are mentioned in the following paragraphs), 2D processing tools were originally developed in order to provide a synoptic view of the study area, highlighting zones where in-depth analyses are necessary and supporting the design of rock slope protection works.

The main steps of the proposed procedure are briefly described below.

2.1. Dip and Dip Direction

By processing a dense point cloud of the slope surface, the orientation of discontinuities at slope scale can be obtained. Dip and dip direction of a discontinuity surface can be calculated by measuring the orientation of a plane interpolating a cluster of points lying on the selected surface. Both semi-automatic [1, 2] and automatic procedures can be applied, according to the level of detail needed.

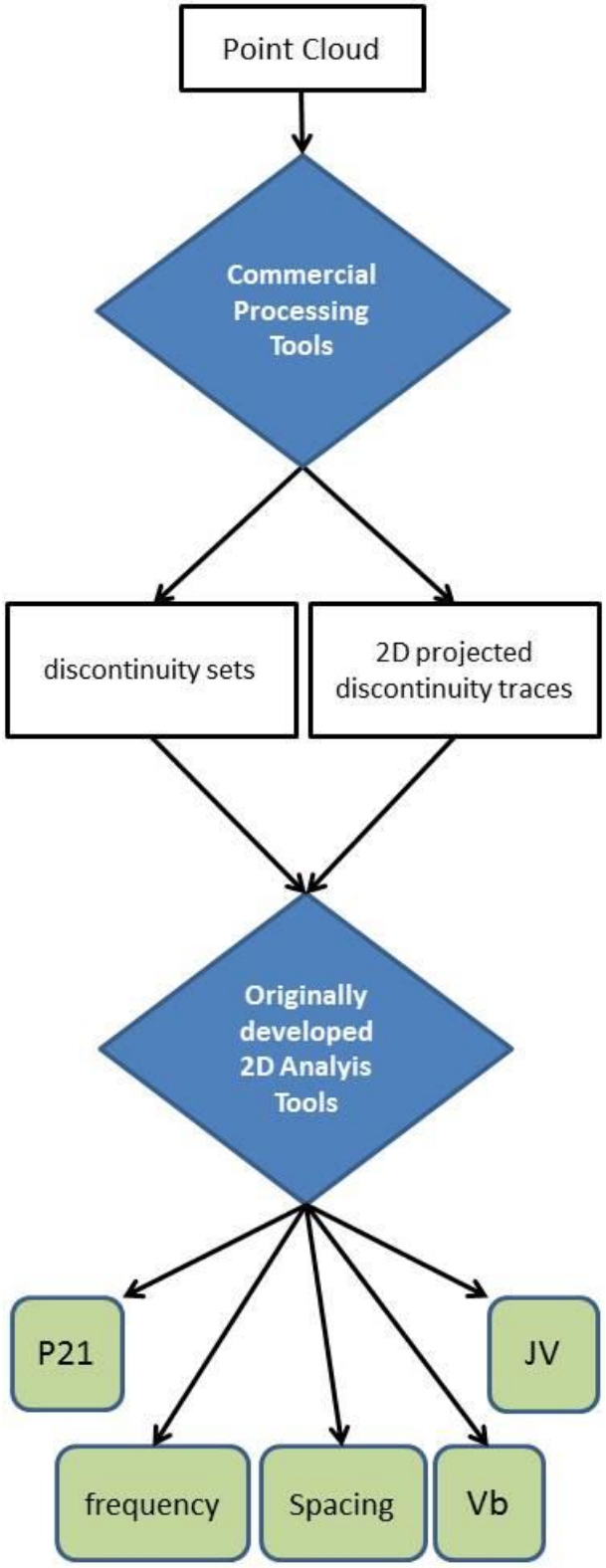

Fig. 3. Processing workflow.

Since the last few years, many commercial automatic processing tools have been released, e.g. Coltop3D [3], developed at the Lausanne University and distributed by Terr@num SàRL (www.terranum.ch). Using the orientation of each single point, a TLS data set can be represented by a 3D image where each single point has a color defined by the local dip and strike direction (Figure 9). In fact this software exploits the idea of having a unique color for both dip and dip direction of a discontinuity plane by adapting a computer graphics classical Hue Saturation Value (HSV) wheel to a standard stereonet [3]. The attitudes referred to every point are related to the normal vectors calculated referring to a circular plane interpolating a point neighbourhood defined by user.

Hundreds of attitude data are then extracted and can be processed with a commercial software (e.g. DIPS by Rocscience Inc., www.rocscience.com) in order to contour orientation data on the stereonet and extract the average orientation of significant joint sets from raw input data.

2.2. 2D analysis for fracture spacing and intensity

Fracture spacing isn't commonly provided by commercial software tools as well as 1D to 3D fracture intensity measurements. Such parameters are the most important in defining the degree of fracturation of the rock mass, even if the least well characterized. Some authors proposed [4, 5] a 3D approach for the evaluation of various intensity indices starting from a digital photogrammetric survey of the rock slope surface. The proposed approach is very challenging, but can't be applied to produce raster maps with the distribution of fracture intensity parameters, which is the target of this work. For this reason we decided to develop proper tools operating in GIS environment, starting from the identification of fracture traces.

We can reasonably assume that curvature changes of the DSM (Digital Surface Model) correspond to fracture traces when projected onto a vertical plane with the average orientation of the slope surface. GIS packages generally offer tools for curvature analysis. Unfortunately, results are generally provided in raster format, which is not suitable for further 2D analyses of fracture intensity, which require vector data. A vector plot of projected fracture traces can be obtained by applying JRC 3D Reconstructor software (www.gexcel.it). After creating a mesh from the point cloud, a semi-automatic tool to detect "Ridges" (prominent mesh edges) and "Valleys" (reentrant mesh edges) is applied to the meshed data. Ridges and valleys are edges shared by mesh's triangles. Each edge can be associated to a curvature value, depending on the angle between the two associated triangles. A threshold on the curvature filters out the smoother edges and leaves only the steeper ones. The edge extraction procedure can be controlled by user for what concerning the curvature, the horizontality, the length of edges and the gaps between them. Ridges and valleys can be then saved as polylines and exported to GIS.

An automated procedure has been implemented (using both ESRI-arcpy and ogr-gdal open source spatial libraries) to perform an iterative calculation of the main geomechanical parameters of discontinuity traces. Before starting processing, a ROI (Region-Of-Interest) is defined and divided into adjacent circular observation windows, with radius set by the user. The observation window formulas [6] are then applied.

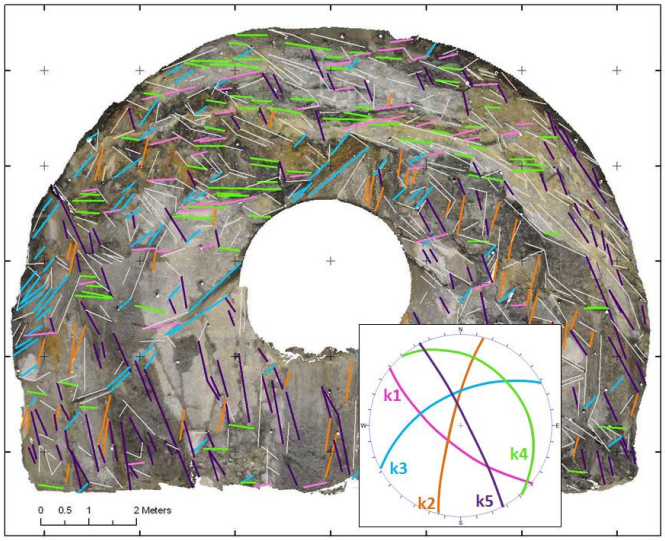

Fig. 4. Fracture traces obtained after processing a TLS scan of a tunnel face, classified according the apparent dip angle. A pilot tunnel is visible.

In the first step the traces of discontinuities (3D polylines) extracted from the laser or photogrammetric model of the survey area are projected onto a view plane, thus becoming 2D polylines, and then simplified in order to highlight the main structures. After data preprocessing, traces are classified on the basis of their apparent angle and grouped according to the main discontinuity set orientation (Figure 4). Discontinuities which do not belong to any known set are grouped into a unique class for further verification. After filtering, remaining classified traces are iteratively analyzed, in order to calculate for each observation window the following parameters:

- Frequency (for each discontinuity set):
  Frequency of a specified discontinuity set is calculated according to the following formula:

$$\lambda = \frac{\sum l_i}{S_{obs} x \sin\alpha} \qquad [\mathrm{m}^{-1}] \qquad (1)$$

where:
l_i represents the tracelength of each discontinuity belonging to the selected set
S_{obs} is the area of the observation window
α is the angle between the pole of each discontinuity set and the observation window.

- Spacing (for each discontinuity set):
Spacing is calculated as the inverse of the frequency value, as follows:

$$L = \lambda^{-1} \qquad [\text{m}] \qquad (2)$$

- P_{21} is a fracture intensity measure allowing for the definition of fracture frequency without referring to a specific set orientation; P_{21} is measured as the cumulative length of fracture traces divided by the area or the observation window [7] (Figure 5).

$$P_{21} = \sum \frac{l_i}{S_{obs}} \qquad [\text{m}^{-1}] \qquad (3)$$

where:
l_i represents the tracelength of each discontinuity contained inside the observation window
S_{obs} is the area of the observation window

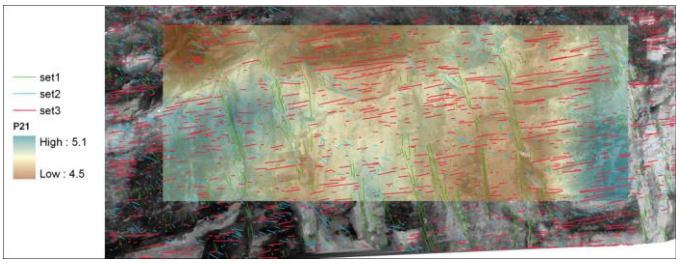

Fig. 5. P21 raster map draped over the orthoimage of a rock cliff; classified fracture traces are also shown.

- Vb is the elementary rock volume, indirectly calculated on the basis of the spacing of three main sets defined by user; several combinations are possible:

$$Vb = \frac{L_1 \cdot L_2 \cdot L_3}{\sin(\gamma_1) \cdot \sin(\gamma_2) \cdot \sin(\gamma_3)} \qquad [\text{m}^3] \qquad (4)$$

where:
L_i is the spacing of the i-esim discontinuity set
γ_i are the angles between each pair of discontinuity sets.

- JV: Volumetric Joint count, calculated as follows:

$$Jv = \frac{1}{L_1} + \frac{1}{L_2} + \frac{1}{L_3} + \ldots + \frac{NR}{5x\sqrt{A}} \quad [\text{m}^{-1}] \qquad (5)$$

where:
NR is the number of "random joints" [8]
A is the area of the observation window

The procedure is totally customizable for what concerns the input parameters; both the grid spacing of the centers of elementary observation windows and the radius of each observation window can be set by user. These two parameters can be set independently, but, to minimize the overlap of adjacent analysis windows and to avoid uncovered areas, the ratio of 1:√2 is usually set.

Finally, data are spatialized and a raster map is obtained for each computed parameter. Raster maps can then be draped over a base layout, e.g. topographic map, orthoimage, online basemap.

As the described parameters are scale-dependent [7], the size of the observation windows has to be carefully set. A sensitivity analysis is strongly recommended before starting processing in order to avoid any wrong evaluation of the rock mass quality. An example will be provided in the following paragraph.

2.3. Slope Mass Rating (SMR) analysis

A second group of tools was implemented in order to calculate a spatialized pattern of the SMR parameter, according to the following formula [9, 10]:

$$SMR = RMR_b + (F1 \cdot F2 \cdot F3) + F4 \qquad (6)$$

where:
RMR_b is the basic Rock Mass Rating [11]
F1 is an adjustment factor related to parallelism of slope and dominant discontinuity
F2 is an adjustment factor related to dip (plane failure) or plunge (wedge failure) of the discontinuity
F3 is an adjustment factor related to relationship between the dip/plunge of the discontinuity (if applicable) and the inclination of the slope
F4 is an adjustment factor related to the method of excavation

Input values are: the DEM of the slope, raster map of RMR_b, raster map of F4 and the orientation (dip and dip direction) of a list of selected sets of discontinuity. The analysis is repeated for each cell of the DEM and each

set of discontinuity and the minimum value of (F1•F2•F3) is chosen.

A raster map is obtained and can be draped over a base layout, e.g. topographic map, orthoimage, online basemap (Figure 6).

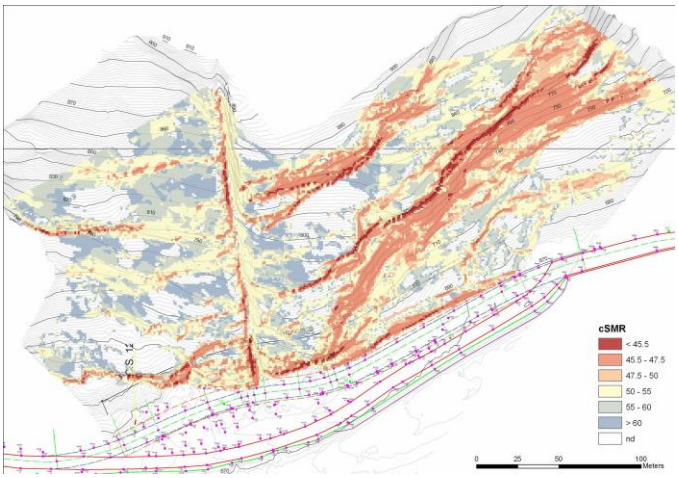

Fig. 6. SMR raster map; a fault crossing the left part of the outcrop is evident.

3. CASE STUDIES

Two case studies are briefly presented.

The first example is a comparison between a map of fracture spacing obtained by applying the automatic approach described in 2.2, and a set of manual spacing measurements carried out along a 15 m long scanline. The overall extent of the ROI is about 680 square meters; the scanline is normal to the discontinuity set represented in the map.

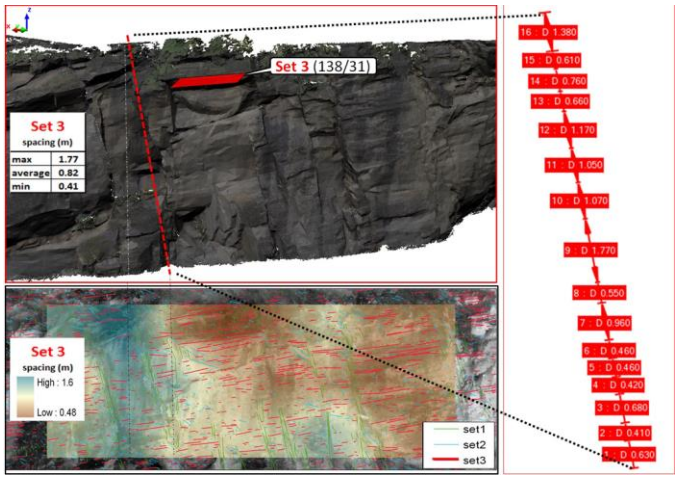

Fig. 7. Case study 1: manual vs automatic spacing measurements (see text for further explanation).

The lower part of Figure 7 shows the raster map of Set 3 spacing value distribution, obtained by applying the previously described 2D analysis tool. The traces of three discontinuity sets are represented with different colors; traces belonging to Set 3 are in red.

In the upper part of Figure 7 a view of the RGB point cloud provided by a terrestrial laser scanner survey is shown; the red dashed line represents the trace of a scanline along which the minimum, maximum and average spacing values for Set 3 were manually measured (single spacing measurements are shown on the right).

The comparison between measured and computed values provided a good fit.

Fig. 8. Case study 2: Matterhorn SW slope around Carrel Hut.

The second example refers to a geomechanical characterization of the rock mass along the Italian normal way to Matterhorn, just below the Carrel Hut (3,830 m a.s.l.), obtained by processing a terrestrial laser scanner point cloud taken from the top of Testa del Leone (3,715 m a.s.l.).

A photo of the area is shown in Figure 8. Two maps of the slope orientation provided by Coltop-3D [3] are presented in Figure 9. Three main discontinuity sets were identified in the study area. Discontinuity traces are shown in Figure 10.

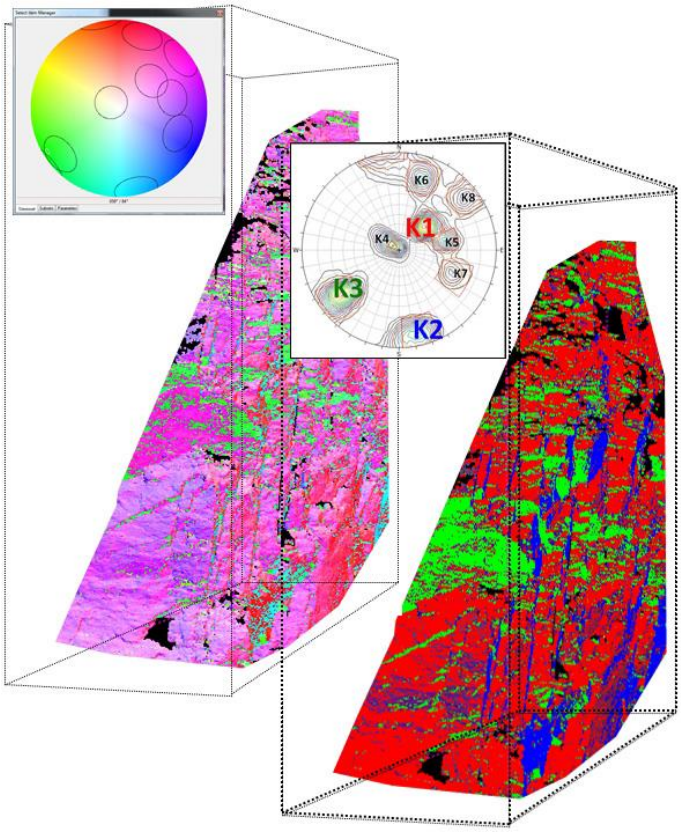

Fig. 9. Case study 2: Slope orientation analysis (left) and orientation of the main discontinuity sets (right).

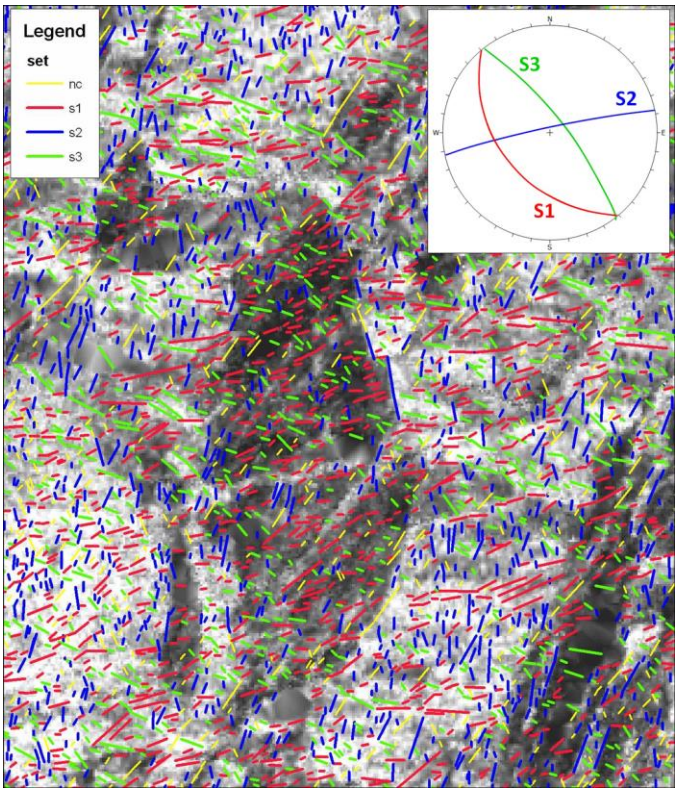

Fig. 10. Case study 2: discontinuity traces grouped according to the orientation of the main sets.

A methodological analysis aimed at identifying the influence of circular observation window radius on the value of fracture intensity is presently under development. In the proposed example, the study area was split into elementary observation windows with radius ranging from 1 to 14 meters. The results are summarized in Figure 11. In this case the results are scale sensitive for small radii (<2 m), different results have been obtained in other sites. At present, our approach includes a preliminary analysis for each case study in order to set the 'optimal radius' of the elementary observation window.

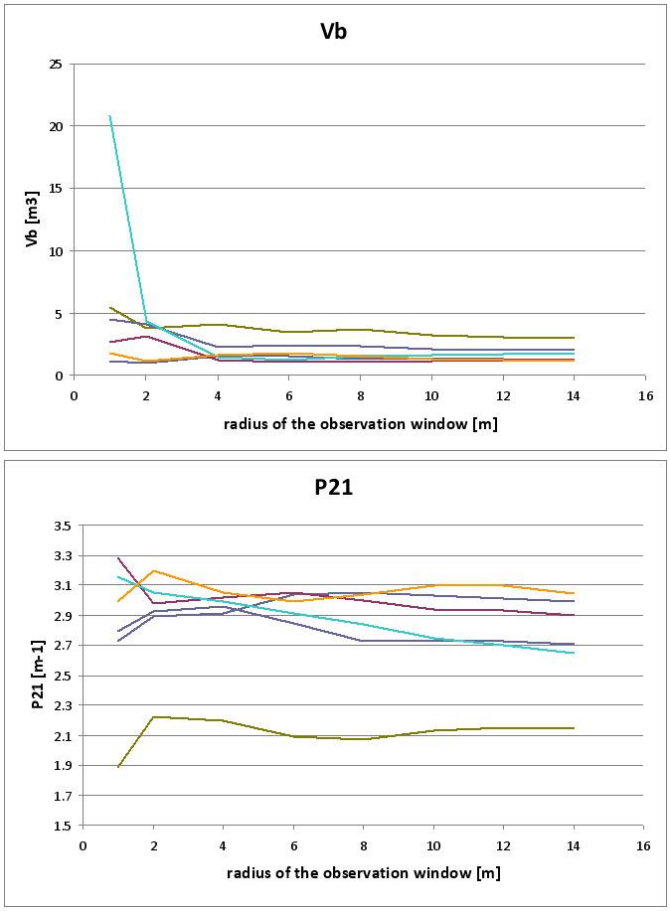

Fig. 11. Case study 2: P21 and Vb values obtained with different radius of circular observation windows.

4. DISCUSSION AND CONCLUSIONS

The procedure for mapping the distribution of significant geomechanical parameters of unaccessible rock cliffs presented in this paper was applied up to now to about ten case studies in the Italian Alps. This helped in highlighting the main advantages and limitations of the proposed approach.

The main advantage is represented by the availability of a continuous distribution of significant geomechanical parameters, which provides valuable help in planning more detailed investigations, designing protection works and defining the most appropriate strategy to monitor slope deformation.

Another advantage is represented by the possibility to study huge areas with a systematic approach, saving time both in field activity and data processing. This could be very effective in such activities as the classification of the rock mass during underground tunnel excavation. Ongoing tests with TLS are providing very encouraging results, demonstrating that the results can be available within a couple of hours after the scan of the tunnel face without need of direct access.

The main limitation is represented by the orientation of fractures with respect to the slope. To this aim, TLS represents a valuable alternative to digital photogrammetry, thanks to the possibility to merge partially overlapped scans taken from different viewpoints. Nevertheless, when moving from the 3D model to the 2D plot of fracture traces obtained by mapping the edges of the 3D surface, some discontinuity sets could become scarcely represented or completely invisible. This must be taken into account when interpreting the results.

Another limitation is the need to manually input some parameters necessary for the rock mass classification, i.e. GSI in the evaluation of RMRb value distribution [9].

At present, semi-automatic tools for RMRb calculation via GSI estimation are under development. As proposed by some authors [12], the estimation of GSI could be obtained from roughness and Vb values. Both these values could be automatically determined starting from geometrical features of the discontinuity sets, which are already standard outputs of the point cloud analysis.

Sensitivity analyses are still in progress in order to test the influence of point spacing and mesh smoothing on the evaluation of discontinuity tracelength, in order to optimize field equipment as well as processing tool configuration parameters.

Finally, the implementation of distributable stand-alone software tools is under development.

AKNOWLEDGEMENTS

The authors are grateful to Antonella Bersani for her useful advice and suggestions.

REFERENCES

1. Broccolato, M., D.G.M. Martelli and A. Tamburini. 2006. Il rilievo geomeccanico di pareti rocciose instabili difficilmente accessibili mediante impiego di laser scanner terrestre. applicazione al caso di Ozein (Valle di Cogne, Aosta). *GEAM, Geoingegneria Ambientale e Mineraria*, XLIII (4).
2. Deline, P., W. Alberto, M. Broccolato, O. Hungr, J. Noetzli, L. Ravanel and A. Tamburini. 2011. The December 2008 Crammont rock avalanche, Mont Blanc massif area, Italy. *Nat. Hazards Earth Syst. Sci*. 11: 3307–3318.
3. Jaboyedoff, M., R. Metzger, T. Oppikofer, R. Couture, M.H. Derron, J. Locat and D. Turmel. 2007: New insight techniques to analyze rock-slope relief using DEM and 3D-imaging cloud points: COLTOP-3D software. In: *Rock mechanics: Meeting Society's Challenges and demands (Vol. 1, e*ds. E. Eberhardt, D. Stead and T. Morrison.. 61-68, Taylor & Francis.
4. Ferrero, A.M., G. Forlani, R. Roncella, I. Voyat. 2009. Advanced geostructural survey methods applied to rock mass characterization. *Rock mechanics and rock engineering* 42 (4): 631-665.
5. Ferrero, A. and G. Umili. 2011. Comparison of methods for estimating fracture size and intensity: Aiguille du Marbrée (Mont Blanc). *Int. J. Rock Mech. Min. Sci.* 48: 1262-1270.
6. Jaboyedoff, M., F. Philippossian, M. Mamin, C. Marro and J.D. Rouillier. 1996. Distribution spatiale des discontinuités dans une falaise. Approche statistique et probabilistique. *Vdf Hochschulverlag AG an der ETH. Zurich.*
7. Dershowitz, W.S. and H.H. Herda. 1992. Interpretation of fracture spacing and intensity. In: *Proceedings of the 33rd U.S. Symposium on Rock Mechanics*, eds. J.R. Tillerson and W.R. Wawersik, 757-766. Rotterdam, Balkema.
8. Palmström, A. 2005. Measurements of and Correlations between Block Size and Rock Quality Designation (RQD). *Tunnels and Underground Space Technology*, 20: 362-377.
9. Romana, M. 1995. A geomechanical classification for slopes: Slope Mass Rating. In: *Comprehensive Rock Engineering*, ed. J.A. Hudson, Pergamon Press.
10. Tomás, R., J. Delgado, J.B. Serón. 2007. Modification of Slope Mass Rating (SMR) by continuous functions. *J. Rock Mech. Min. Sci*, 44: 1062-1069.
11. Bieniawski, Z. 1989. *Engineering rock mass classification*, J. Wiley & Sons.
12. Cai, M, P.K. Kaiser, H. Uno, Y. Tasaka and M. Minami. 2004. Estimation of rock mass strength and deformation modulus of jointed hard rock masses using the GSI system. *Int. J. Rock Mech. Min. Sci.* 41(1): 3–19.